Tellus (1998), 50A, 109–123
Printed in UK – all rights reserved

TELLUS
ISSN 0280–6495

The influence of the mean state on interdecadal variability in flat-bottomed ocean models

By K. ANDREW PETERSON* and RICHARD J. GREATBATCH, *Department of Physics and Physical Oceanography, Memorial University of Newfoundland, St. John's, NF, Canada A1B 3X7*

(Manuscript received 17 December 1996; in final form 18 September 1997)

ABSTRACT

It has been well-demonstrated that many flat-bottomed ocean models possess interdecadal oscillatory solutions. Recently, propagation of viscous (or coarsely resolved) Kelvin waves around the boundary has been implicated in the oscillations. In this paper, we examine how the mean state affects the character of the oscillation. We find that the stratification along the northern boundary has a large effect upon the oscillation. Mean states with an essentially unstratified north-east corner, lead to long period oscillations as the viscous boundary wave slowly crosses the northern boundary. Conversely, mean states with a stratified north-east corner, but unstratified north-west corner, lead to short-period, but larger-amplitude, oscillations since boundary wave propagation is arrested only in the north-west corner. We demonstate that the different character of oscillations under different zonal redistributions of a diagnosed flux are a consequence of the different mean states induced by the redistribution.

1. Introduction

Numerous flat-bottomed ocean models have exhibited decadal scale oscillations in their thermohaline circulation under constant surface flux boundary conditions (Huang and Chou, 1994; Greatbatch and Zhang, 1995; Cai et al., 1995; Chen and Ghil, 1995). Greatbatch and Peterson (1996; hereafter GP) have presented an explanation for these oscillations in terms of the propagation of a viscous Kelvin wave around the model boundaries and the creation of anomalies through disturbances created in the western boundary current by the propagating wave. Even when the viscous boundary layer is not resolved, as is often the case in coarse resolution models, these waves still exist as the numerical boundary waves first noted by Killworth (1985) and discussed in Winton (1996; hereafter W96). Cai et al. (1995; hereafter CGZ) induced oscillations using a zonal redistribution of the surface flux diagnosed from a spin-up experiment. CGZ found that the character of the oscillation changed as they varied the amount of zonal redistribution, finding that the period increased as a more zonally uniform flux was applied and shortened if a negatively redistributed flux was applied.‡ It has been shown in W96 and GP that the lack of stratification along the northern boundary retards the progression of the Kelvin wave and as such is elemental in both setting the decadal time scale of the oscillation and the amplitude. The structure of the stratification along the high latitude boundary can therefore be expected to play an important role in determining the character of the oscillation. In turn the high latitude stratification is closely linked to the structure of the mean state. Furthermore, GP found an oscillation under a diagnosed flux,

* Corresponding author.
email: drew@crosby.physics.mun.ca

‡ Negative redistribution increases the east/west variation in the flux.

demonstrating that zonal redistribution of the flux is not necessary for the development of an oscillation. We will show in this paper, through the use of various predetermined mean states, that it is the stratification along the northern border, and the associated mean state, that determines the character of the oscillation that develops. This applies both to oscillations under a diagnosed flux and to oscillations under a zonal redistribution of a diagnosed flux. Indeed, the different character of the oscillations under different zonally redistributed fluxes is attributed to the different mean states under the different surface flux fields.

The simple idealized model used in this study is intentional. Previous studies (Greatbatch and Zhang, 1995) have shown that this type of oscillation is present in both temperature-only models and models that include both temperature and salinity forcing. Furthermore, the oscillations exist in similar forms (GP) whether the surface forcing is constant flux on both temperature and salinity, or constant flux on salinity with a restoring boundary condition on temperature (mixed boundary conditions). Thus in this study we use the simpler temperature-only model in order to make the dependence on the mean state more easily identifiable. The use of a flat-bottomed model is also important. Winton (1997) and Greatbatch et al. (1997, unpublished*) have shown that including variable bottom topography in a model can lead to damping of oscillations on an interdecadal time scale as energy leaks from the baroclinic to the barotropic mode. By using a flat-bottomed model we avoid this complication and concentrate on the effect of the mean state alone. The special nature of flat-bottomed models should be taken into account when attempting to relate our results to observations.

The plan of this paper is as follows. In Section 2 we describe the model and diagnostics used. In Section 3 we describe an oscillation using a mean state spun up under a zonally uniform restoring temperature. Sections 4 and 5 discuss oscillations with mean states that have been spun up with restoring temperatures possessing a warm northwest and warm north-east sector respectively. Section 6 then points out the similarity to results from experiments driven by zonally redistributed fluxes. Section 7 presents a summary and conclusions.

* Manuscript title: Interdecadal variability in a coarse resolution model with North Atlantic bottom topography.

2. Model and experiment description

The model and model setup used for these experiments are identical to that used in GP. The model employs a single tracer (temperature) and uses a 4000 m flat-bottom with 14 levels in the vertical. It is 60° in longitudinal width and extends from 5°N to 65°N with 2.4° grid resolution in both directions. The model is run with uniform values for the horizontal diffusivity and viscosity of $10^3\ m^2\ s^{-1}$ and $10^5\ m^2\ s^{-1}$ respectively. Similarly, the vertical diffusivity and viscosity are uniform at $10^{-4}\ m^2\ s^{-1}$ and $10^{-3}\ m^2\ s^{-1}$ respectively. No wind forcing is employed, and the salinity is held constant at 35 p.s.u., density being calculated using a realistic equation of state similar to that of Bryan and Cox (1972). Deep convection is carried out by employing a large vertical diffusion ($10^5\ m^2\ s^{-1}$) whenever the water column is unstably stratified and iteratively solving the diffusion equation until the water column becomes stable.

To demonstrate the significance of the mean state, we have spun up the model employing a surface restoring boundary condition and five different restoring temperatures that differ in the location of the minimum temperature. The restoring temperatures used for the spin-up of Experiments 1, 2 and 3 are shown in Figs. 1a–c, respectively. The restoring temperature profiles for Experiments 4 and 5 are obtained by an east/west flip of Figs. 1b,c so that the minimum temperature is in the northwest corner. At the end of each spin-up, when the model is in equilibrium, a corresponding heat flux is diagnosed from the restoring boundary condition over a 50 year period. This flux is then used to drive the model, the initial condition being the end state of the spin-up and all other model parameters remaining unchanged. When run under the diagnosed flux, all experiments result in regular oscillations of various characteristics, a summary of which is reported in Table 1. The experiments were integrated under the diagnosed flux for at least 1000 model years, by which time all experiments had undergone several periods of steady oscillations.

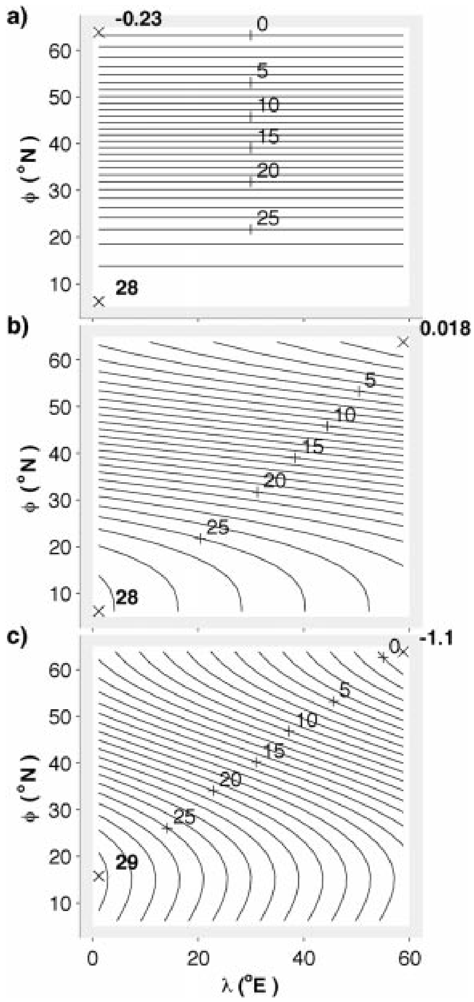

Fig. 1. Restoring conditions used for the various experiments. Contour interval is 1°C with the location of maximum and minimum values identified with an ×.

Fig. 2 shows for each oscillation the time evolution of the kinetic energy, the maximum value of the meridional overturning streamfunction, and the overturning streamfunction at the point that undergoes the largest anomaly. In all experiments, this latter point is located one grid box away from the northern boundary.

The five experiments all have different mean states, each with its own mean flow characteristic. With each mean state comes differing locations and extents of the areas with little or no stratification. This in turn will mean that any boundary wave will be arrested at different points along the northern and/or eastern boundary producing the differing character of oscillation.

Table 1. *The model experiments*

Experiment no.	Period (years)	Mean KE (10^{-2} J m^{-3})	KE Range (10^{-2} J m^{-3})
1	29.8	4.13	2.80
2	39.4	4.39	3.21
3	34.8	4.15	1.43
4	18.1	4.07	3.83
5	16.4	3.60	3.27
6	34.4	4.10	2.83
7	21.7	4.12	3.10
8	35.1	4.31	3.01
9	21.1	4.26	3.61

A useful diagnostic for these experiments is the baroclinic pressure defined by (GP)

$$P = p - \frac{1}{H}\int_{-H}^{0} p\,\mathrm{d}z, \tag{1}$$

where

$$p = g\int_{z}^{0} \{\rho - \bar{\rho}(z')\}\,\mathrm{d}z'. \tag{2}$$

$\bar{\rho}(z)$ is a reference density field that depends only on the vertical coordinate, z, and is usually taken to be the density averaged horizontally over the model domain and averaged in time over several oscillation periods. Since P is the baroclinic pressure, it has zero vertical average. It should be noted that because we do not include wind forcing, the barotropic flow in our model is very weak. As a consequence, the horizontal gradients of P are a very good approximation to the horizontal gradients of the total pressure, and henceforth we shall refer to the baroclinic pressure simply as the pressure.

3. Oscillations resulting from a spin-up using a zonally uniform restoring temperature

For our standard case, Experiment 1, where the spin-up restores to a temperature that is zonally uniform, we obtain an oscillation with period of 30 years. In the course of one oscillation, some portion of the northern boundary is always completely unstratified, which means that the propaga-

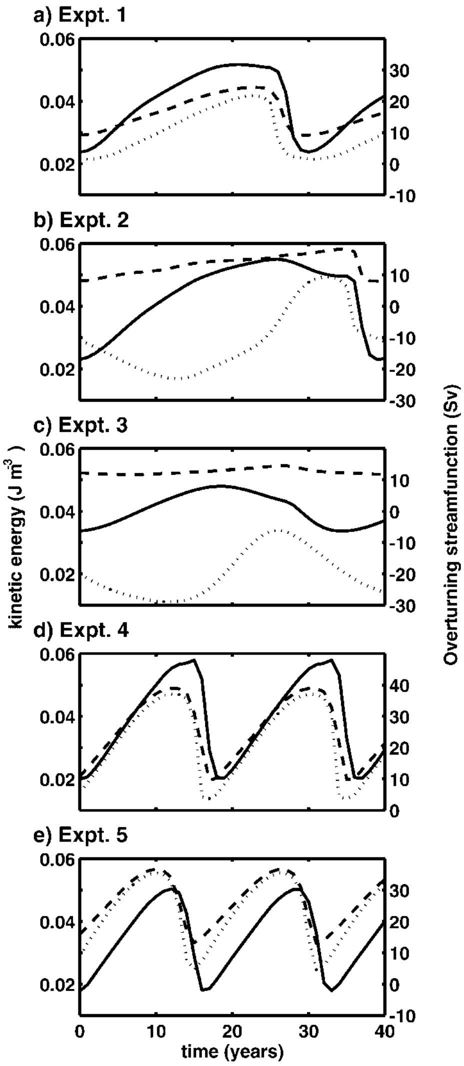

Fig. 2. Time series of a typical oscillation for Experiments 1–5. Plotted are time series of the kinetic energy (solid line, left axis), the maximum value of the overturning streamfunction (dashed line, right axis, 1 Sv $= 10^6$ m^3 s^{-1}), and the value of the overturning streamfunction at the point undergoing the largest anomaly (dotted line, right axis). For all experiments, this latter point is always a point adjacent to the northern boundary.

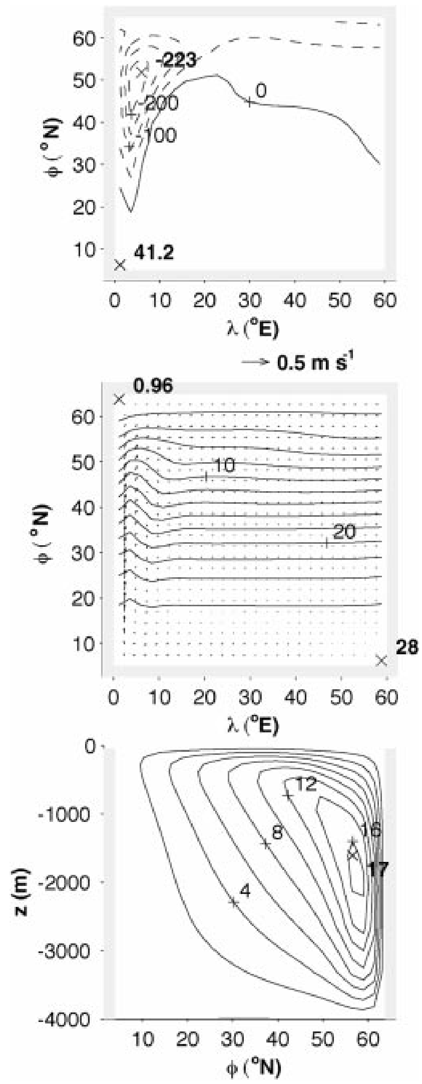

Fig. 3. The time mean state of Experiment 1 averaged over many oscillations. (a) The flux used to drive the model, contour interval of 50 W m^{-2} with the maximum and minimum values (in W m^{-2}) displayed with an ×. (b) The time mean surface temperature, contour interval 2°C, with the maximum and minimum values (in °C) identified with an ×. Also included is the time mean velocity field. A scaling arrow of 0.5 m s^{-1} is included above the plot. (c) The time mean overturning streamfunction, contour interval 2 Sv with the maximum value (in Sv) identified with an ×.

tion of a viscous Kelvin wave along this boundary will be severely arrested. Fig. 3 shows the mean state averaged over several oscillations. We see that, except for the influence of the western boundary current, the mean surface temperature is primarily zonal in structure and possesses a one-celled overturning streamfunction that peaks near the northern boundary.

We begin describing the oscillation when the kinetic energy is at a minimum, which roughly corresponds to the point when the maximum of the surface pressure anomaly is in the north-west corner, producing an anomalous flow that is maximally opposed to the western boundary current. This is year 0 in the series of snapshots shown in Fig. 4. Fig. 4 shows the anomalous surface pressure (left column) and the temperature adjacent to the boundary (right column) at several times during a typical oscillation of Experiment 1. At year 0 of the oscillation, the western regions of the northern boundary are stratified (Fig. 4, time 0, right column), meaning the wave propagation is fairly rapid around the north-west corner at this time. This can be seen in the pressure contours along the northern and western boundaries in the left column of Fig. 4 at time 0, all of which have a down wave slant along these boundaries. This implies that the high pressure anomaly in the north-west corner is being quickly leaked out around the boundary, and indeed, only one year later, the west, south, and much of the eastern boundary are all under positive pressure anomaly, the wave being stopped along the north end of the eastern boundary by the lack of stratification there. This situation persists for the next several years. By our next snapshot at year 11, we see the high pressure anomaly has been completely removed from the north-west corner. This transfer of the high pressure from the western to eastern boundaries, is accompanied by an increase in the maximum overturning streamfunction, this being related to the east/west pressure difference (see GP). By year 11 the western boundary current is being pushed away from the western boundary (as is clear from the anomalous geostrophic flow being produced by the anomalous pressure at this time), pushing the warm water into the interior, and producing a colder, more unstratified north-western boundary, in addition to producing the start of a high pressure anomaly in the interior. This is the advective part of the oscillation. In these 11 years there has been little progression of the high pressure front up the eastern boundary, as the wave propagation at the northern end of this boundary is extremely slow. Indeed it is not until year 19 that the zero anomalous pressure contour reaches the north-east corner. By our next snapshot at year 21, the zero anomaly contour has moved part-way across the northern boundary. At this time, the northward flow (as exemplified by the overturning streamfunction evolution shown in Fig. 2a) is nearing its maximum, and furthermore, the anomalous flow is now directed into the northern boundary, leading to the build-up of stratification along the northern boundary. The first evidence of this is barely discernable in the right column of Fig. 4, year 21, but is more obvious at year 25. Since the build up of stratification is behind the pressure front, the gravity wave speed there is greater than the gravity wave speed ahead of the front. This in turn leads to a build up of the high pressure front, as can be seen by the fact that the maximum of the kinetic energy has just been passed at year 20 and the maximum in the overturning, representative of the largest east/west pressure difference, is about to be reached at year 22 (Fig. 2a). Furthermore, the kinetic energy is at, or near to, its maximum value during the time that the pressure front is propagating along the northern boundary. At our next snapshot in year 25, the high pressure front has reached the north-west corner, and most of the northern boundary has become stratified. The shape of the contour lines in the north-west corner still display signs of slow propagation speeds, but that is about to change since by the next year the front will reach stratified waters and start to rapidly propagate down the western boundary. Indeed, in five short years, the overturning and kinetic energy will have collapsed completely, and the cycle will repeat itself.

4. Oscillations obtained with an unstratified north-east corner

In Experiment 2, the oscillation results from the spin-up under the restoring temperature in Fig. 1b, which has a cold north-east sector and a warm north-west sector. Unlike our other cases, the oscillation that results here did not simply come from a switch to flux conditions. In fact, the switch to flux conditions did not lead to oscillations. Rather the oscillation was produced by initializing with the final temperature field from the spin-up but with the velocity field set to zero. With this initial condition, the model was run forward in

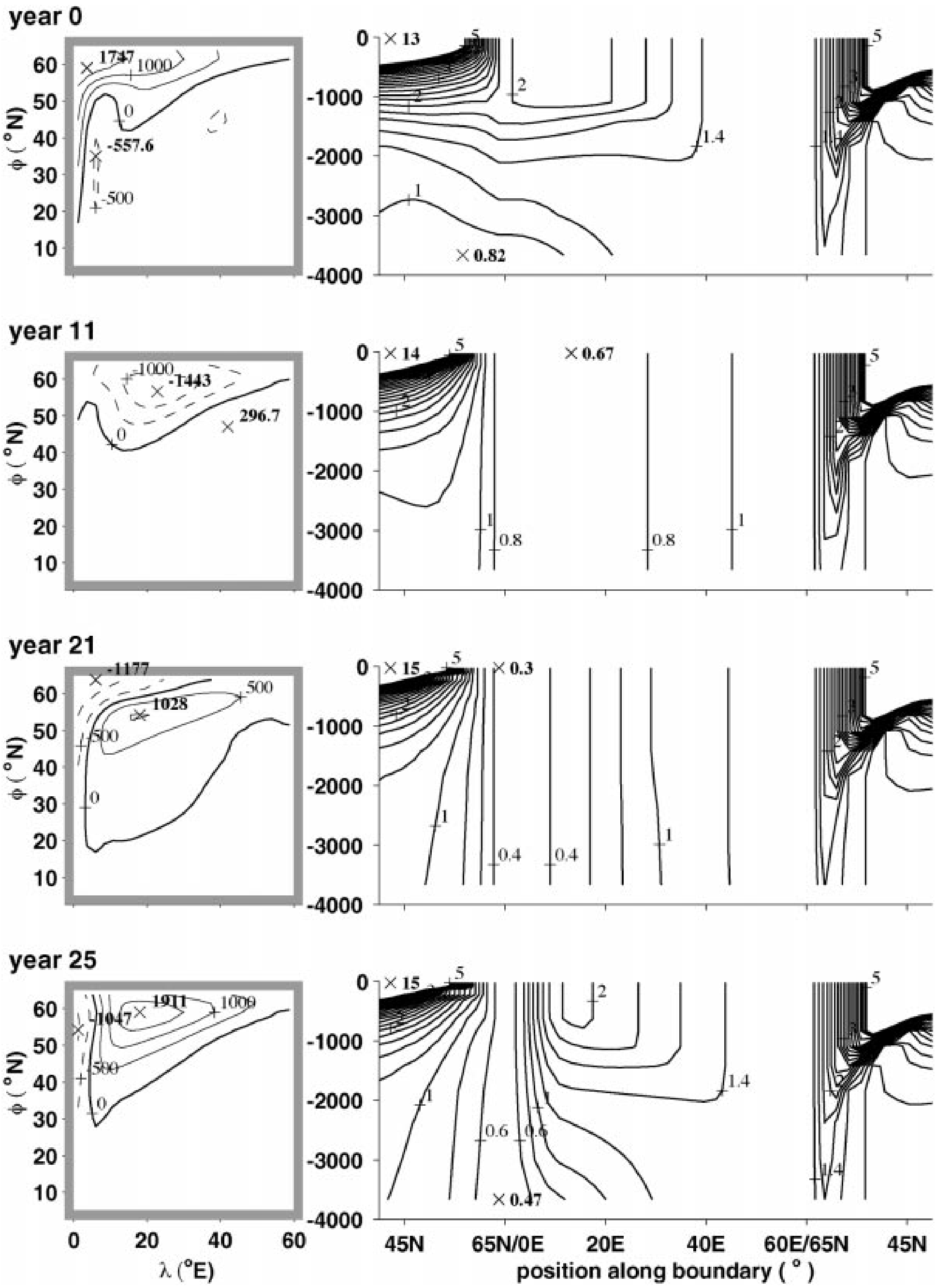

Fig. 4. Snapshots of the anomalous surface pressure (left column) and the temperature in the first grid box adjacent to the boundary (which is folded out) for Experiment 1. The pressure contour interval is 500 N m^{-2} with the solid lines being positive contour values and the dashed lines being negative contours values. The temperature contour interval is 0.2°C. Contours of temperature above 5°C are not displayed. The maximum and minimum values (in °C) are displayed and identified with an ×.

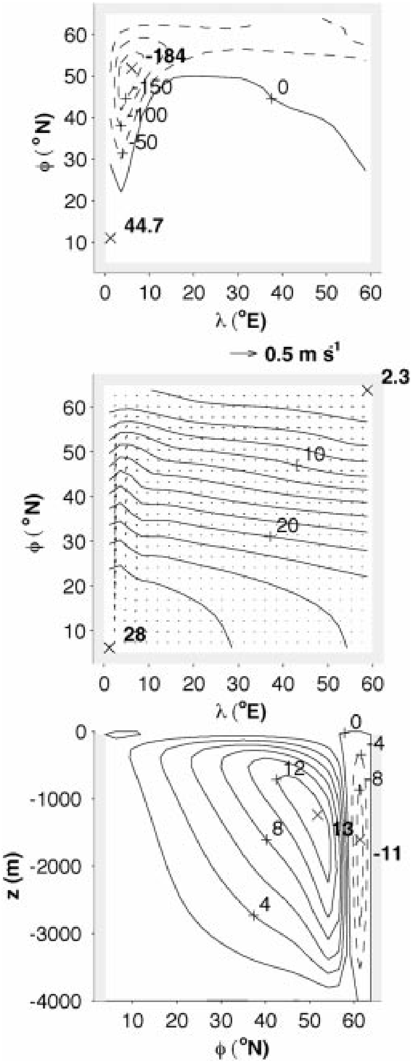

Fig. 5. As Fig. 3, but for Experiment 2. (c) Contour intervals of the negative (dashed) values of overturning streamfunction are 4 Sv, and the minimum value (in Sv) is identified with an × in addition to the maximum value.

time under the diagnosed flux, and the velocity field allowed to establish itself as part of the integration. A regular oscillation of period 39 years results. The mean state produced under this oscillation is shown in Fig. 5. We see that the mean surface temperature is representative of the restoring temperature used in the spin-up. In addition, one sees that the overturning has a two cell structure. The maximum positive overturning occurs at about 52°N, and north of about 58°N a robust negative cell exists. This negative cell exists for all but years 28 through 35 of the oscillation. In this experiment, one has for much of the oscillation a lack of stratification along the eastern half of the northern boundary, but stratification along the western half of the boundary. This can be seen in the series of time snapshots of temperature adjacent to the boundary shown in the right column of Fig. 6, the equivalent of Fig. 4, but for Experiment 2.

Again we begin the description of the oscillation at the point when the kinetic energy is a minimum. This is year 0 in the series of snapshots in Fig. 6. At this time, the high pressure anomaly is over stratified portions of the boundaries and is being quickly propagated around the basin until it reaches the unstratified regions in the north-east corner. At this time the anomalous flow is opposed to the western boundary current, and the north-west corner is at the start of a cooling trend. The next snapshot is at year 16, by which time the high pressure anomaly has almost completely been leaked out of the north-west corner and a high pressure front has been formed along the eastern boundary where a lack of stratification does not allow for its quick progression. Also during this period, the anomalous flow has been so weakened that a low pressure anomaly of cold water has been built up across most of the northern boundary and northern interior. During this period, the value of the low latitude (below 58°N) overturning streamfunction has been increasing (Fig. 2b, dashed line). Meanwhile as the high pressure anomaly is slowly displaced westward along the northern boundary, being replaced by the low pressure anomaly, the value of the high latitude overturning streamfunction slowly decreases (Fig. 2b, dotted line), indicating a strengthening of the reverse cell at high latitudes, reaching a minimum value at year 12. Progressing to the next snapshot at year 28, we see that the zero contour dividing the high and low pressure anomalies on the eastern boundary has finally moved up and around the north-east corner, having reached the corner at about year 26. It is the increased time that it has taken for this to happen and the increased time it takes for the front to move across the eastern portion of the northern boundary that is responsible for the increased period of oscillation when compared with Experiment 1. This is primar-

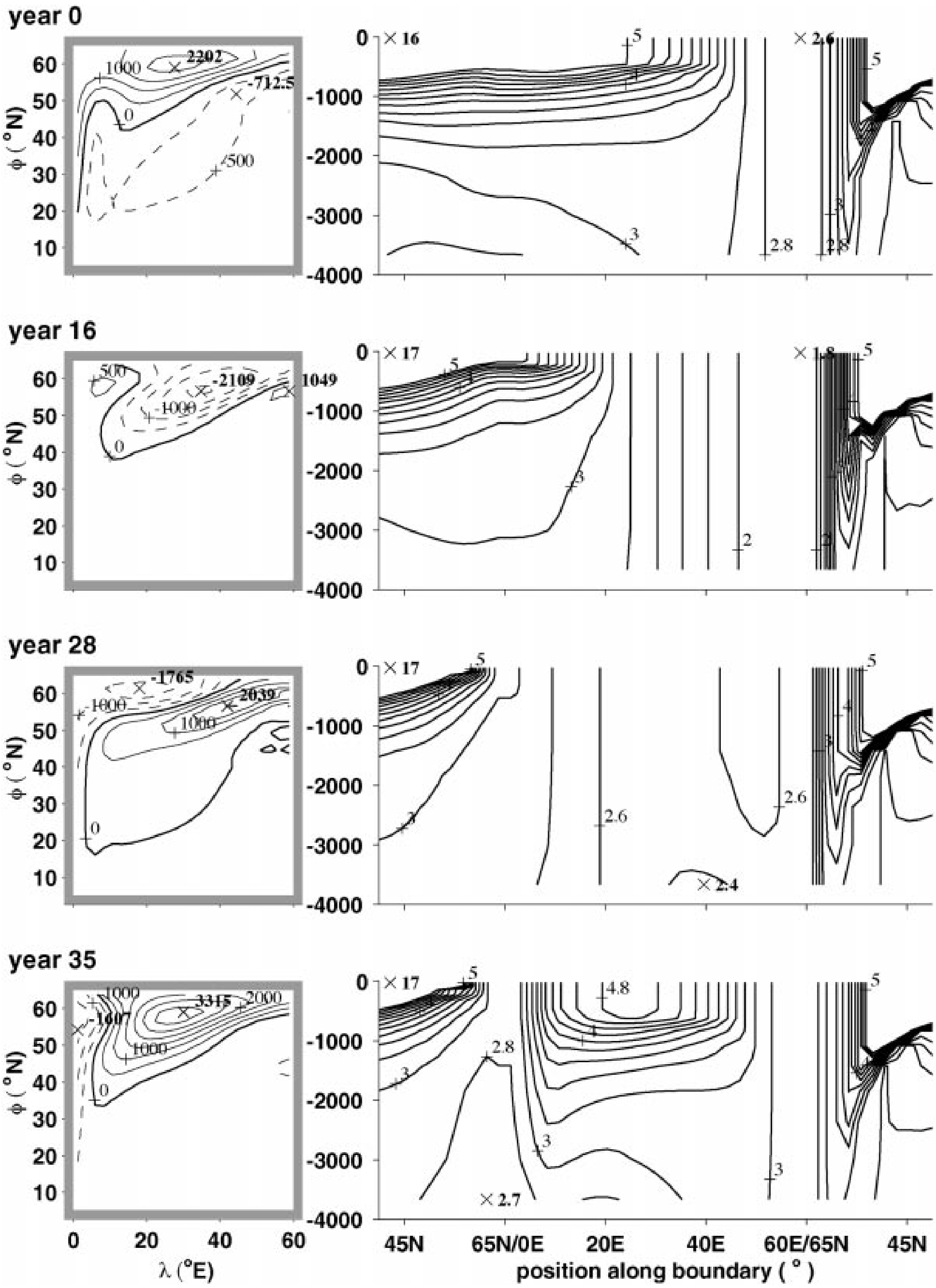

Fig. 6. As in Fig. 4, but for Experiment 2.

ily due to the lack of stratification in this corner, making the wave propagation extremely slow there. By year 28, the east/west pressure difference produces positive values of the overturning streamfunction at all latitudes, and the kinetic energy has just passed it maximum value at year 26 (Fig. 2b). Finally, at this time, the anomalous flow is directed toward the north-east corner, transporting warm waters to the north-east corner, warming and stratifying those waters, as can be seen in the boundary temperature snapshot at this time. At the same time, the cooling trend in the north-west corner is beginning to destratify that corner. One can also see that the advection of warm waters by the increased north and north-eastward flow has produced a significant high pressure anomaly in the interior extending into the north-east corner, resulting in a positive feed-back whereby increased north/north-east flow leads to larger pressure anomalies and plays a role in propagating the anomalies along the boundary (W96; GP). The last snapshot is at year 35 of the oscillation, at the time when the value of the overturning streamfunction is at a maximum and the kinetic energy has briefly plateaued from a gradual decline. At this point the anomalous flow is directed into the north-west corner, stratify-ing those waters. One can now see the effects of the increased wave speed on the high pressure front, as the zero contour now has a definite curvature down wave and is beginning to pull away from the high pressure anomaly maximum, situated near the middle of the northern boundary. In 4 more years, the kinetic energy will again be at its minimum, and the cycle will repeat itself.

Experiment 3 is spun up under the restoring condition of Fig. 1c. This experiment produces an oscillation with a shorter period (35 years) than Experiment 2, despite the fact that it is a more extreme example of moving the low temperature, unstratified water to the north-east corner. The difference here is that now the north-west corner is so warm the stratification never weakens there, allowing the boundary wave to easily leak out down the western boundary. In the end, this means that a shorter time is required for the pressure front to move across the northern boundary, leading to the shorter oscillation period. It is also responsible for the rather small amplitude of this oscillation, as the leakage from the north-west corner does not allow for as big a build up of amplitude. This is also exemplified by the rather weak secondary peak in the kinetic energy that occurs here (Fig. 2c). This peak, or in this case, merely an inflection point in the kinetic energy decline at year 28, occurs as the pressure front reaches the north-west corner. In the case of Experiment 2, this is an unstratified boundary at that time, resulting in a strong front and the significant plateau in kinetic energy. In Experiment 3 the north-west corner is stratified so the front is rather weak as it passes this point.

5. Oscillations obtained with a stratified north-east corner

In contrast, Experiment 4, spun up under the restoring condition given by an east/west flip of Fig. 1b, produces a mean state with a warm north-east sector, not unlike the warm north-west sector of the previous discussion. This case oscillates with a period of 18 years and the mean state of the oscillation is shown in Fig. 7. This case has a one cell overturning with considerably more strength than in Experiment 1 owing to the larger east/west pressure difference brought about by the slanted temperature profile.

Fig. 8 shows the series of snapshots similar to those in Fig. 4, but this time for Experiment 4. As usual year 0 is the minimum in the kinetic energy. We see that at year 0 almost all of the northern boundary is stratified, and as a result, the wave propagation is quite rapid around the basin. At our next snapshot at year 6, the north-west bound-ary has already cooled and destratified. As a result, the low pressure anomaly has become stuck in this vicinity and the high pressure anomaly has already progressed around most of the basin and is now at about the mid-point of the northern boundary. Notice, unlike the other two cases, this oscillation has completely skipped the north-east corner. This corner is stratified, so the viscous boundary wave quickly passes over this area. This is responsible for the short-period of this oscilla-tion, as the whole oscillation is essentially confined to the north-west corner. Notice that at year 6 the zero contour intersecting the northern boundary still has a significant down wave bend, representa-tive of the stratification in the north-east sector. By the next snapshot at year 12, the maximum value in the overturning streamfunction has

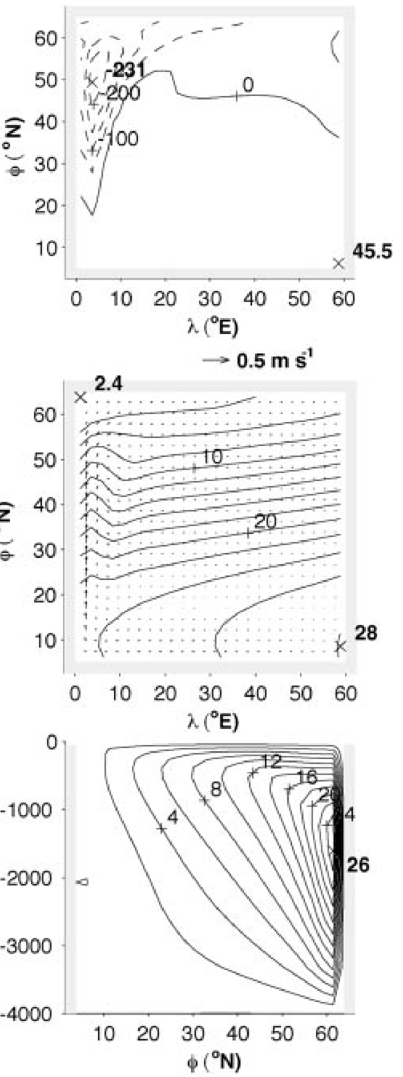

Fig. 7. As in Fig. 3, but for Experiment 4.

already been reached. The southward propagating low-pressure anomaly leads to the large east/west pressure difference associated with the maximum of the overturning streamfunction. Also in part responsible for the east/west pressure difference is the large interior high pressure anomaly that can be seen in this snapshot. This anomaly is caused by the advection of warm southern waters into the interior by the western boundary current. The conditions for large overturnings will be short lived as the low-pressure anomaly has already encircled most of the boundary, and will quickly round the stratified north-east corner, as is seen by our last snapshot at year 15. At this point, both the head of the high pressure anomaly and the tail of the low pressure anomaly are stuck over the unstratified waters of the north-west corner. This leads to the biggest build up of the front between the two anomalies in the northwest corner, resulting in large contributions to the kinetic energy (at this point, the anomalous pressures are maximally set up to contribute to the western boundary current). However, since the head of the low pressure anomaly has already rounded the north-east corner, by this point the east/west pressure difference is already declining, and thus so is the overturning. Soon after this snapshot, both anomalies hit stratified waters, so first the low pressure anomaly clears out from the western boundary, followed in quick succession by the high pressure anomaly's rapid propagation around the basin, leading back to the snapshot of year 0.

Experiment 5 is spun up under the restoring temperature of the east/west flip of Fig. 1c. As expected, this case is just a more extreme case of Experiment 4. Here the period is even shorter (16.4 years), as the region in which the boundary wave propagation is held up is confined to an even greater extent to the western end of the northern boundary.

6. Zonal redistribution

In this section, we briefly report on the results of two zonal redistribution experiments in order to show the similarities to the results described above. These experiments were performed by a zonal redistribution of the flux diagnosed from the restoring condition of Fig. 1a. Here the redistributed flux is given by

$$Q = (1\text{-}\alpha)\ Q_{\text{diagnosed}} + \alpha Q_{\text{zonal}}, \tag{3}$$

$Q_{\text{diagnosed}}$ being the diagnosed flux, Q_{zonal} being its zonal average, and α is a parameter that determines the amount of zonal redistribution.

In Experiment 6, the model was driven with a flux redistributed by $\alpha = 1$. The initial state is the end state of the spin-up of Experiment 1. A regular oscillation results with period of 34 years. Similarly, Experiment 7 is driven by a negative

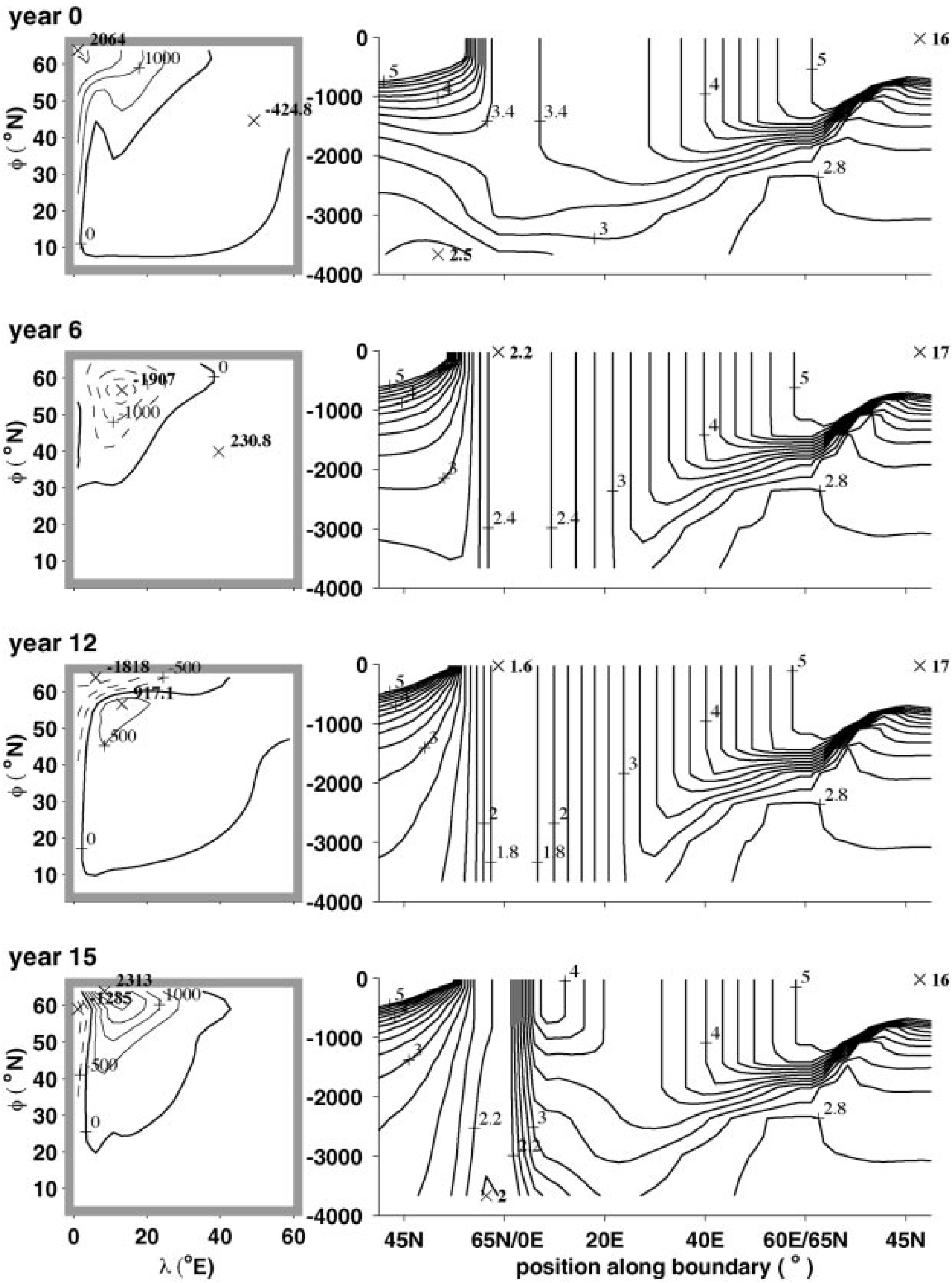

Fig. 8. As in Fig. 4, but for Experiment 4.

redistribution of the flux with $\alpha = -0.4$. Here one obtains an oscillation with period 22 years. The mean state of Experiment 6 is similar to the mean states of Experiments 2 and 3, as can be seen by comparing Figs. 9b and c with Figs. 5b and c. Similarly, the mean state of Experiment 7 (Figs. 10b,c) is similar to the mean states of Experiments 4 (Figs. 7b,c) and 5. The time evolution of the kinetic energy and the overturning streamfunction are shown in Fig. 11 for Experiments 6 and 7 and are similar to the same time evolutions shown in Fig. 2 for Experiments 2/3 and 4/5 respectively. In particular, it should be noted that although the flux used to drive Experiment 6 (Fig. 9a) lacks the zonal structure of the surface flux used to drive Experiment 2 (Fig. 5a), the oscillation characteristics of the two experiments are very similar. This supports our claim that it is only the mean state that is relevant for determining the character of the oscillations.

In Experiment 6, the kinetic energy has two very distinct peaks similar to Experiment 2. Indeed, the second peak is more pronounced in Experiment 6. This is the peak in kinetic energy that occurs as the high pressure front reaches the north-west corner. It is larger and more pronounced in Experiment 6 since the stratification in this area weakens more than in Experiment 2 or 3 owing to the warmer north-west corner that is applied in those experiments. Thus in Experiment 6 it is more difficult for the boundary wave to leak out the high pressure anomaly than in Experiments 2 and 3. This results in the second peak seen in Experiment 6 as the high pressure front reaches the north-west corner.

Experiment 7, the negative redistibution experiment, is very much like Experiments 4 and 5. Here, as expected, the period is dramatically shorter (22 years) than Experiment 1. In addition, the shape of the kinetic energy and overturning evolution is much the same as in Experiments 4 and 5. Here the period is a little longer, as the north-east corner in the case of Experiment 7 is not as warm and stratified as it was in the case of Experiments 4 and 5.

In our last set of experiments we perform two spin-ups in which the surface temperature is restored to the mean surface temperature of Experiments 6 and 7, respectively. That is the restoring fields are the temperature fields shown in Figs. 9b and 10b. As usual, once a condition of equilibrium is reached, a flux is diagnosed from

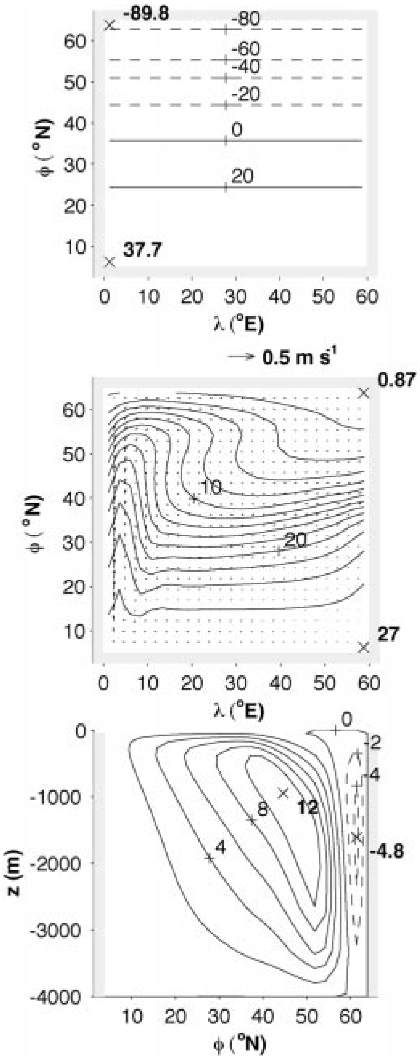

Fig. 9. As in Fig. 3, but for Experiment 6. (a) Contour interval is 20 W m^{-2}. (c) Negative contours are displayed with dashed lines, and the minimum value (in Sv) is displayed with an $\times$ in addition to the maximum value.

the restoring spin-up, and this flux is used to drive the model. This is an attempt to show once again that it is only the mean state of the system that is responsible for the character of the oscillation. Here we expect that Experiment 8 should yield an oscillation almost identical to Experiment 6, whilst Experiment 9 should yield an oscillation almost identical to Experiment 7, despite the fact that both these latest experiments are driven by a

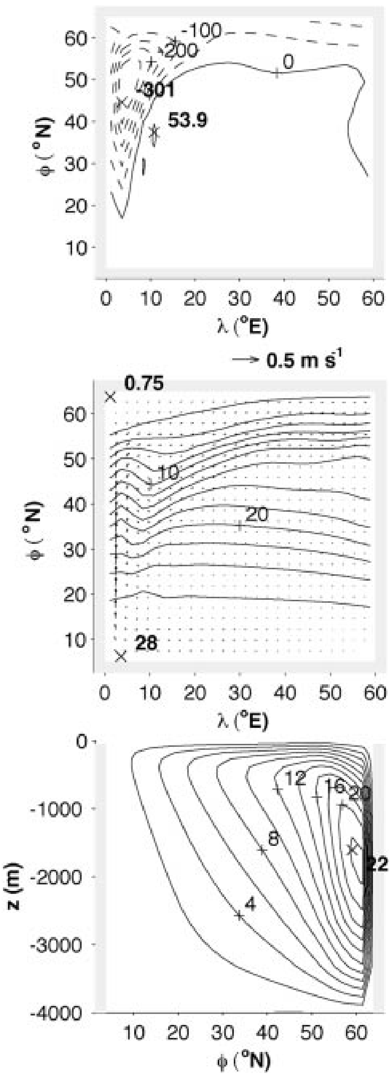

Fig. 10. As in Fig. 3, but for Experiment 7.

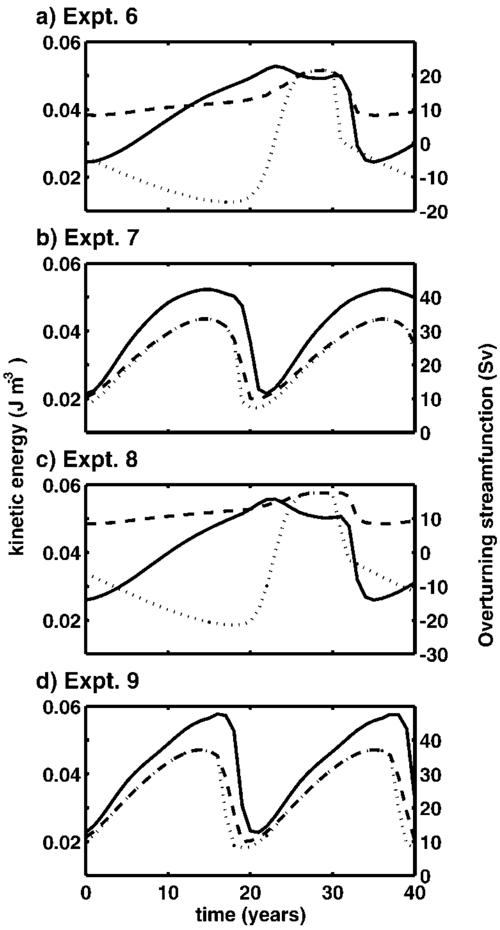

Fig. 11. As in Fig. 2, but for Experiments 6 through 9.

diagnosed flux and not a flux that has been redistributed. As one can see from Fig. 11, this is indeed the case. In the case of Experiment 8, the oscillation is almost identical to that of Experiment 6. For Experiment 9, the oscillation is again almost identical to that of Experiment 7.

7. Summary and conclusions

Interdecadal variability in ocean models is a topic of considerable interest of late. Work has been undertaken using flat-bottomed, coarse resolution models in order to try and understand some of the underlying mechanisms. Recently, progress has been made in the realization that viscous Kelvin wave (or their numerical equivalent) propagation around the basin boundaries is a fundamental aspect of the oscillations in flat-bottomed models (GP; W96). The complicating feature of this particular wave, which results in the decadal scale of the oscillations, is that a significant portion of the wave propagation is over unstratified or weakly stratified waters along the northern and north-eastern boundaries. Since the wave speed depends upon the strength of the stratification, this severely arrests the wave propagation, resulting in the decadal time scales that are observed in the oscillation. Furthermore, the amplitude build up is also due to the lack of stratification. As the high pressure front moves across the northern boundary, it produces an anomalous flow toward the boundary that brings warm southern waters to the boundary stratifying the boundary behind the front. Ahead of the high pressure front the boundary is typically unstratified. Thus there are large gravity wave speeds behind the front and slow gravity wave speeds ahead of the front, resulting in a situation that promotes wave amplitude growth.

Until now, little attention has been focused on how the mean state of the model ocean might affect the oscillations. CGZ found that their experiments would oscillate only after their flux had been redistributed. They thus attributed the existence of oscillations to the existence of a mismatch between the surface forcing condition (or implied atmospheric heat transport) and the oceanic heat transport. Furthermore, the character of their oscillations were very different under different redistributions of the surface flux. In this paper, we have demonstrated that the character of the oscillation can be explained through the effect the mean state has on the boundary wave, and thus the oscillation. By changing the character of the surface flux, one also changes the character of the mean state. For instance, applying a positive redistribution of the flux increases heat loss in the north-east corner and decreases heat loss in the north-west corner, producing a mean state that has a cold unstratified north-east corner and a warm stratified north-west corner. A negative redistribution of the flux has exactly the opposite effect.

We have performed 2 sets of experiments with a cold north-east sector and warm north-west sector, and two sets with a warm north-east sector and cold north-west sector. In addition, we have also a standard case with a mean state that is essentially zonal in surface temperature distribution. As expected, these new mean states did produce oscillatory solutions much like that which might have been expected from previous zonal redistribution experiments. The two cases with a cold north-east sector produce an oscillation with a longer period than the standard case. This is due to the fact that the boundary wave takes a longer period to negotiate the northern portion of the eastern boundary and the eastern portion of the northern boundary than it takes in our standard case. In addition, the double peak character of the oscillation in the kinetic energy can be traced to this boundary wave first reaching the north-east corner and then later reaching the north-west corner. Indeed, the prominence of this second peak in the north-west corner can easily be traced to the conditions in that corner, the more stratified that corner being, the quicker the wave passes through, and the less prominent this peak.

In contrast, the oscillations that occur when the north-west corner is cool and weakly stratified and the north-east corner is warm and well stratified are extremely simple. Here the boundary wave only gets impeded in the north-west corner, greatly reducing the period of the wave. Almost all observable characteristics of the oscillation are limited to the north-west corner.

It is quite apparent that the mean state, and in particular, the abundance and location of weakly stratified areas along the boundary is the determining factor in the character of oscillation that develops. We have found that decadal oscillations in flat-bottomed ocean models are sensitive to conditions along the northern and north-eastern boundaries. Since in general, these boundaries are poorly resolved, and are a poor representation of the physical boundaries present in the real ocean, this casts doubt on the relationship between interdecadal variability found in flat-bottomed coarse resolution models and any observed climate or oceanographic variability. In fact, as noted in the introduction, it is also known that including a continental shelf leads to damping of oscillations at the interdecadal time scale (Winton, 1997; Greatbatch et al., 1997, unpublished), suggesting that the importance of correctly representing this slope in models. Further research is required using higher resolution studies that also properly resolve the coastal wave guide.

8. Acknowledgements

Funding from NSERC and AES in the form of a Science Subvention award, and a grant from the Canadian Institute for Climate Studies, is gratefully acknowledged. The authors would also like to acknowledge two anonymous reviewers for contributing several useful comments.

REFERENCES

Bryan, K. and Cox, M. D. 1972. An approximate equation of state for numerical models of the ocean circulation. *J. Phys. Oceanogr.* **2**, 510–514.

Cai, W., Greatbatch, R. J. and Zhang, S. 1995. Interdecadal variability in an ocean model driven by a small, zonal redistribution of the surface buoyancy flux. *J. Phys. Oceanogr.* **25**, 1998–2010.

Chen, F. and Ghil, M. 1995. Interdecadal variability of the thermohaline circulation and high-latitude surface fluxes. *J. Phys. Oceanogr.* **25**, 2547–2568.

Greatbatch, R. J. and Peterson, K. A. 1996. Interdecadal variability and oceanic thermohaline adjustment. *J. Geophys. Res.* **101C**, 20 467–20 482.

Greatbatch, R. J. and Zhang, S. 1995. An interdecadal oscillation in an idealised ocean basin forced by constant heat flux. *J. Climate*, **8**, 81–91.

Huang, R. X. and Chou, L. 1994. Parameter sensitivity study of the saline circulation. *Clim. Dyn.* **9**, 391–409.

Killworth, P. D. 1985. A two-level wind and buoyancy driven thermocline model. *J. Phys. Oceanogr.* **15**, 1414–1432.

Winton, M. 1996. The role of horizontal boundaries in parameter sensitivity and decadal-scale variability of coarse-resolution ocean general circulation models. *J. Phys. Oceanogr.* **26**, 289–304.

Winton, M. 1997. The damping effect of bottom topography on internal decadal-scale oscillations of the thermohaline circulation. *J. Phys. Oceanogr.* **27**, 203–208.